Proceedings of the 17th World Congress
The International Federation of Automatic Control
Seoul, Korea, July 6-11, 2008

CPG Based Motion Control for an Underwater Thruster with Undulating Long-Fin

Xiang Dong, Shuo Wang, Zhiqiang Cao, Min Tan

Laboratory of Complex Systems and Intelligence Science, Institute of Automation, Chinese Academy of Sciences, Beijing 100080, China; (e-mail: {dong, swang, zqcao, tan}@compsys.ia.ac.cn).

Abstract: A CPG based motion control approach is proposed for a biologically inspired underwater thruster with undulating long-fin. The characteristic of rhythmic motion patterns generated by CPG suits well to control the thruster, which has multiple fin rays coupled by membrane. Based on modified Matsuoka model, an artificial CPG controller consisting of ten neural oscillators with sensory information feedback is built. A novel method for phase control of the output signals is brought forward to make it possible to control and regulate the output of the coupled oscillators on-line. The experiment shows the CPG controller is valid to generate thrust by controlling the long fin.

1. INTRODUCTION

In the oceans which cover approximately 71% of Earth's surface, fish is one kind of amazing creatures. Comparing to traditional artificial underwater vehicles, it has advantages of greater efficiency and better maneuverability. Therefore, a lot of studies have been conducted to the propulsive mechanisms of fish to design novel underwater vehicles. According to Webb's classification (Sfakiotakis et al., 1999), the fish's swimming type can be generally divided into two categories: BCF locomotion, which generates thrust by bending fish's body into a backward-moving propulsive wave that extends to its caudal fin, and MPF locomotion, which develops alternative swimming mechanisms that involve the use of their median and pectoral fins. As the former locomotion can achieve greater thrust and accelerations, it has been employed in the majority researches of biomimetic underwater vehicles. However, MPF locomotion has the advantages of greater maneuverability and better propulsive efficiency, especially at slow speeds, and attracts more and more attention. This paper will introduce an underwater thruster with undulating long-fin which is inspired by gymnotiform (one form of MPF locomotion) fish and the experiment platform of the thruster.

Central pattern generator (CPG) is a neural circuit that is capable of producing rhythmic motion patterns. The approach of implementing CPG for locomotion control arises from the research of animals' rhythmic movements and has been successfully applied to several kinds of biomimetic robots (Delcomyn, 1980; Bradley et al., 1997; Hu et al., 1999; Ijspeert et al., 2007). As the swimming of gymnotiform fish depends on the rhythmic undulating movements of its rays, it's a good choice to apply CPG model to the motion control of the thruster with undulating long-fin. There are many kinds of CPGs with different types of coupled oscillators (Izumi et al., 2006). Among these, Matsuoka oscillator has been widely used because of its properties of simple mathematic expression and explicit biological significance (Kimura et al., 2005; Matsuoka, 1985). In this article, we adopt modified Matsuoka model to build a CPG controller comprising ten neural oscillators. The controller gets feedback signals from sensors to alter the locomotion mode of the thruster.

The rest of the paper is organized as follows. In section 2, we introduce the underwater thruster and the experiment platform. In section 3, we first give the modified Matsuoka model, then present the CPG based controller and interpret the method of phase selection. In section 4, an experiment is carried out to switch the locomotion modes based on sensor's feedback. In section 5, we summarize our work.

2. THE UNDERWATER THRUSTER AND THE EXPERIMENT PLATFORM

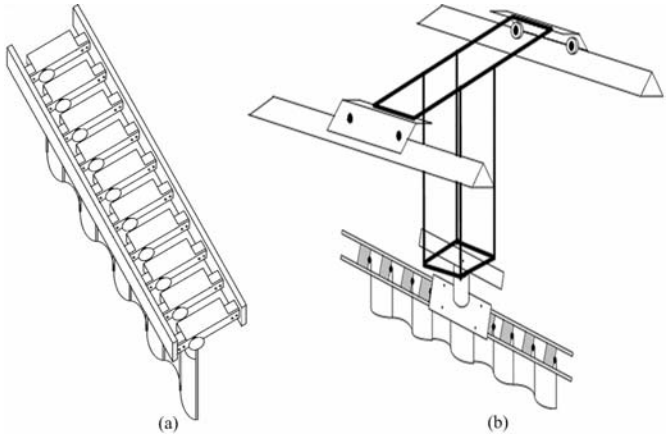

Fig. 1. Sketch of the underwater thruster and the experiment platform: (a) The underwater thruster; (b) The experiment platform mounted with the thrusters.

The underwater thruster is composed of ten servo motors which are fixed by supporting brackets and connecting blocks. The servo horn of every motor mounts a slender cylindrical copper vertical to the output axis of the motor. A piece of elastic membrane whose width is same with the length of the

copper connects all the coppers together. Through coordinated control of these motors, the thruster transfers momentum to the surrounding water by passing traveling waves, thus gets thrust for locomotion. The mechanical rate of working and the swimming speed can be modulated by changing the shape and speed of these traveling waves (Lighthill et al., 1990).

The experiment platform is designed for fixing the thruster and serving as a test bench while be mounted with sensors. It consists of two parallel triangular tracks, a hanger and a fixed board. The thruster is connected to the fixed board by a ball bearing. This structure allows the thruster moves along the tracks and rotates around the mounting axis. The sketch map of the thruster and the experiment platform is shown in Figure 1.

3. CPG BASED CONTROLLER

3.1 Neural Oscillator and CPG Model

The oscillator adopted here is modified from the Matsuoka model. It has a minor difference with Kimura's improved model in that the output is not obtained from sigmoid function but directly from the status variables. Thus it has smooth output signal.

Figure 2 describes the neural oscillator (NO). It consists of two mutually inhibiting neurons, which is represented by the following nonlinear equations:

$$\begin{cases} T_r \dot{u}_i^f + u_i^f = bv_i^f + ay_i^e + \sum_{j=1}^{n} w_{ij} y_j^f + c_i + d_i, \\ T_a \dot{v}_i^f + v_i^f = y_i^f, \\ T_r \dot{u}_i^e + u_i^e = bv_i^e + ay_i^f + \sum_{j=1}^{n} w_{ij} y_j^e + c_i - d_i, \\ T_a \dot{v}_i^e + v_i^e = y_i^e, \\ y_i^{f,e} = \max(u_i^{f,e}, 0), \\ y_i = u_i^f - u_i^e. \end{cases} \quad (1)$$

where $i = 1, 2, \cdots, n$ denotes the i[th] oscillator, the superscript e, f denote an extensor neuron and a flexor neuron of oscillator. u_i^e, u_i^f denote the inner state of an extensor and a flexor neuron of the i[th] oscillator respectively. v_i^e, v_i^f are variables representing the degree of the self-inhibition effect of the neuron. y_i^e, y_i^f are the outputs of extensor and flexor neurons. The quantities T_r and T_a are time constants of $u_i^{e,f}$ and $v_i^{e,f}$. a is a connecting weight between flexor and extensor neurons. b is a constant representing the degree of the self-inhibition influence on the inner state. c_i and d_i are external inputs with constant values. w_{ij} is a connecting weight between neurons of the i[th] and j[th] NO. y_i denotes the output signal of the i[th] oscillator.

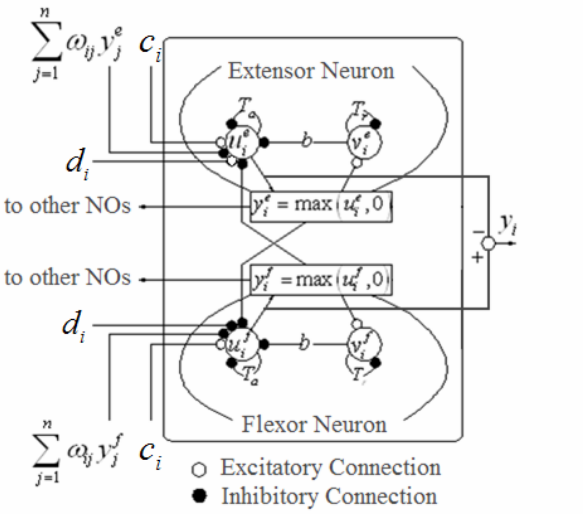

Fig. 2. Neural oscillator.

The CPG model we built includes ten neural oscillators. Each oscillator corresponds to a motor. These oscillators are coupled with each other via connecting weight matrix W, as illustrated in Figure 3, and produce stable oscillating signals for the control of the motors.

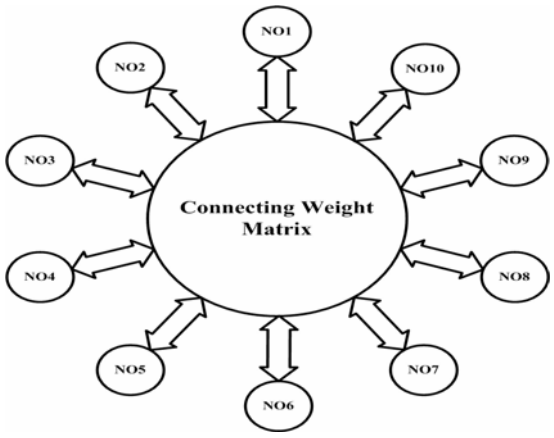

Fig. 3. CPG model with ten neural oscillators.

The output of the CPG model is get from the numerical solution of equation (1). In discrete time series, the solution of one interval is set as the initial data of the next interval. In this way, discrete output series can be obtained.

As the CPG model uses sigmoid function to form feedback item, it has a characteristic of strong nonlinearity. The relations between the parameters and the output are not explicit and can only be determined by experiments. (Zhang , 2004) gives some characteristics:

1) Frequency of output signals is mainly determined by parameters T_r, T_a. For the purpose of keeping the amplitudes

of output signals of CPG during changing parameters T_r and T_a, T_r and T_a must be in certain proportion.

2) The magnitudes of CPG output signals are mainly determined by parameter c_i.

3) The parameter d_i affects the bias of the output to x axis. And when the ith d_i alters to a larger scale, the state of output will be changed from oscillation to stabilization.

3.2 A Method for Phase Control

The characteristics introduced above can be used to generate proper waves for the control of the motors. However, there is still an important issue to be solved, that is, the problem of output signals' phase control.

In CPG model, the phase of the output signal is mainly affected by the initial data of oscillators' state variables. Previous work (Hu et al., 1999; Ijspeert et al., 2007; Zhang, 2004) adopt random methods for the selection of the initial data, that is, choosing random values in a small region around the origin o for the initial data. However, this method can not determine the phase of the output signals. When the oscillators reach the stable state, the phase relations of the output signals are non-determinate. They have to be judged offline to be used for the control of objects. It may not be a big problem for the control of biped or quadruped robots, which just have two or four neural oscillators. But for the thruster presented in this paper, as it adopts ten oscillators, the judgment is considerably difficult. As a result, an online method should be developed.

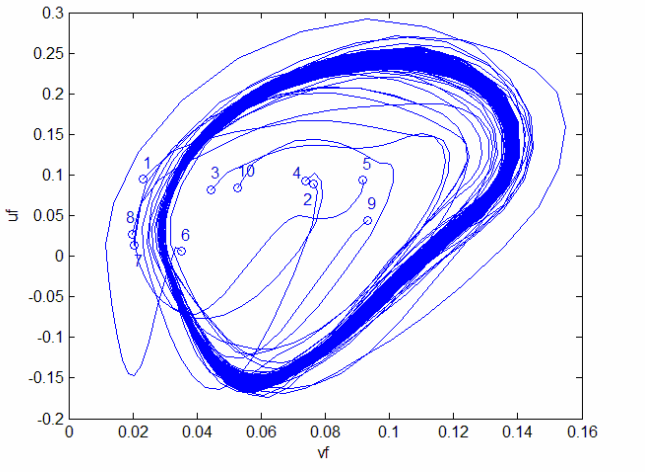

Fig. 4. Limit cycle of the state variables with random initial data.

The phase relations among the neuron oscillators are considered firstly. In the state variable space of the neuron oscillators, the distribution of the initial data used in random methods is stochastic. As illustrated in Figure 4, the state variables, thus the oscillators, converge to a limit cycle, but the phase relations among each other are turbid. Therefore, selection of the initial data should contain the information of phase relations to make these data distribute regularly.

The relations among the state variables within an oscillator can not be neglected, too. It's hard to get explicit relations from the equations of the neural oscillator. So we turn to observe the state variables map. Figure 5 shows the state variables u^e, v^e, u^f, v^f of an oscillator arriving at stable state which comes from a random method. From the map, we can see that u^e and u^f have an excursion of about $T/2$ on phase, and v^e and v^f have approximate $T/8$ phase lead respectively corresponding to u^e and u^f, where T is the oscillating period. On amplitude, v^e and v^f are about one-fourth of u^e and u^f.

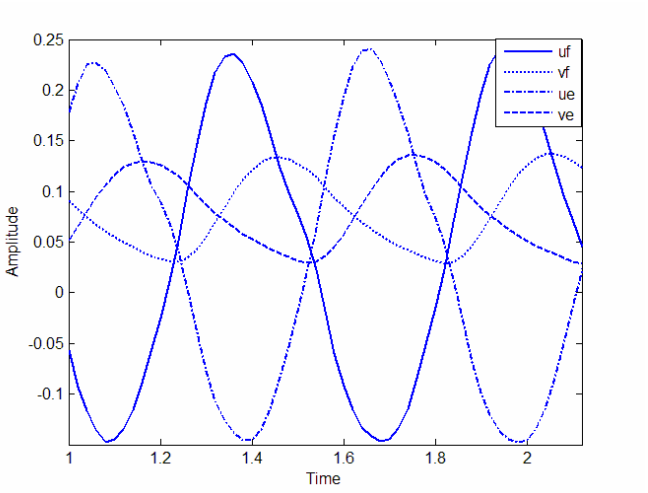

Fig. 5. The oscillating waves of the state variables.

By employing a periodic function similar to the oscillating wave in shape, formalized equations can be obtained for the choosing of the initial data. The form of the equations is as follows:

$$\begin{cases} u_{0i}^f = a_1 + b_1\Phi\left(\dfrac{(i-1)}{n}T\right) \\ v_{0i}^f = a_2 + b_2\Phi\left(\dfrac{(i-1)}{n}T - \theta_1\right) \\ u_{0i}^e = a_1 + b_1\Phi\left(\dfrac{(i-1)}{n}T + \theta_2\right) \\ v_{0i}^f = a_2 + b_2\Phi\left(\dfrac{(i-1)}{n}T + \theta_2 - \theta_1\right) \end{cases} \tag{2}$$

where $i = 1, 2, \cdots, n$ denotes the ith oscillator, n is the total number of the oscillators, Φ denotes the periodic function, a_1, a_2, b_1, b_2 are parameters corresponding to the bias and the amplitude of the oscillating waves, T is the period of the function and θ_1, θ_2 are the phase difference.

In our studies, sine function is taken as Φ and T is set to 2π without loss of generality. Other parameters need not be precisely valued. They can be changed in a certain arrange and will eventually converged to stable values. With new initial data, the convergence of the stable variables is shown in Figure 6, and the output signals of the CPG model are shown in Figure 7.

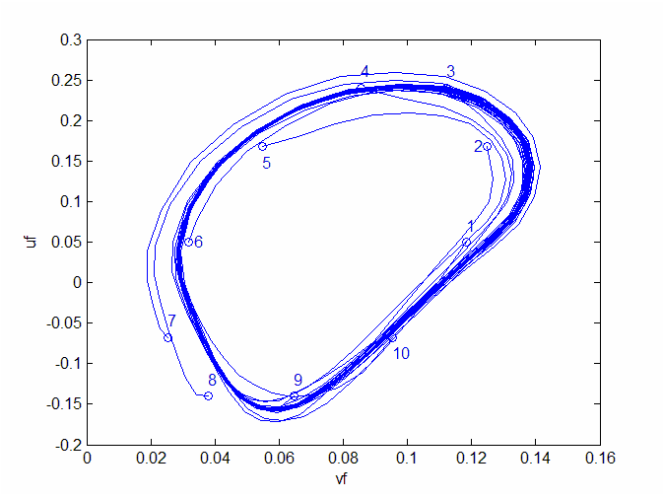

Fig. 6. Limit cycle of the state variables with tuned initial data.

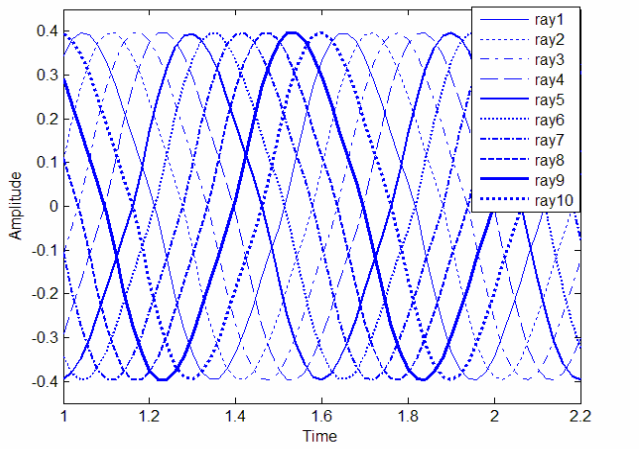

Figure. 7. The output signals of the CPG model.

3.3 CPG Based Controller

Based on the CPG model, a controller has been developed. It consists of three parts: a decision layer, the CPG model and a PWM generator. The decision layer gets feedback signals from the sensors and receives commands from the external, then tunes the parameters of the CPG model to generate different locomotion modes. The CPG model produces signals for the oscillating angles of the motors. And the PWM generator transforms the angle signals to pulse-width modulation (PWM) signals for the control of the motors. Then the controller sends PWM signals to the motors to drive the thruster. Sensors are mounted on the experiment platform to send back the sensing information, such as the distance of the obstacles or the velocity of the thrusters, to the controller.

The controller, the thruster and the sensors make up a close-loop control system. The sketch map of the system is shown in Figure 8.

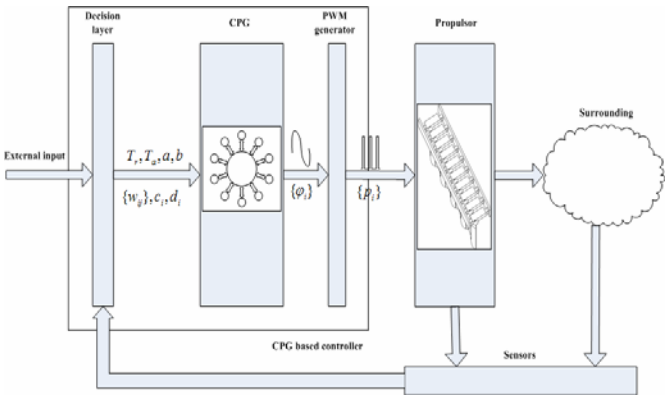

Fig. 8. The sketch of the CPG based control system

4. THE EXPERIMENT

4.1 introduction of the experiment

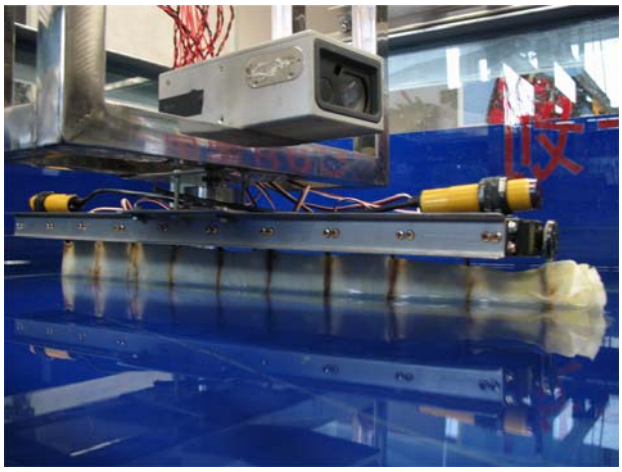

Fig. 9. The thruster mounted with a distance laser sensor and two infrared sensors

In order to validate the effectiveness of the CPG controller, an experiment is carried out to switch the locomotion modes of the thruster based on the feedback signals of two infrared sensors and a distance laser sensor. The experiment is done in a water tank with a length of 1.8 meters and a width of 1 meter. The infrared sensors are fixed on the front side and back side of thruster, along the direction of the thruster's movement. The effective detecting range of the infrared sensor is from 5 centimeters to 30 centimeters. The distance laser sensor is mounted at the bottom of the hanger, just being on top of the thruster. Real time distance information from the platform to the sidewall of tank is get with an interval of 0.4s. The thruster mounted with sensors is shown in Figure 9.

The experiment is designed like this: the thruster starts to move from a rest state in the middle of the tank. When it comes near to the sidewall of the tank, the infrared sensor

detects obstacle and the thruster switches from forward swimming mode to braking mode. When the velocity of the thruster reduces to 0, the thruster switches to backward swimming mode. While in the process of the movement to the other side of the tank, the thruster changes its undulating frequency and amplitude. Same as the situation mentioned above, the thruster brakes near the sidewall, then switches to the forward swimming mode. When the thruster moves to the middle of the tank, it switches to rotational mode.

4.2 Generation and switch of locomotion modes

As it is mentioned in section 3.1, the frequency, amplitude and bias of output oscillating wave of the CPG model can be tuned by changing the parameters of the model. The relations between the parameters of the CPG model and the characteristics of the output oscillating waves are illustrated in Figure 10. By varying the values of T_r, c_i and d_i, the characteristics of the output wave change and different locomotion modes can be obtained.

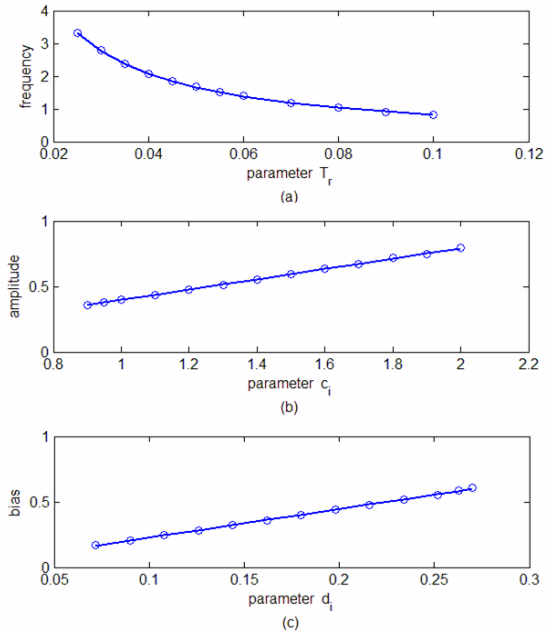

Fig.10. Relations between the parameters of the CPG model and the characteristics of the output oscillating waves: (a) relation of parameter T_r and frequency of the output wave; (b) relation of parameter c_i and amplitude of the output wave; (c) relation of parameter d_i and bias of the output wave.

The locomotion modes can be generally divided into three categories: regular swimming mode, braking mode and rotational mode. And the regular swimming mode can be delicately divided into forward swimming mode and backward swimming mode.

The regular swimming mode requires a stable forward or backward propagating traveling wave, with steady frequency and amplitude. The phase differences among the rays should be fixed. The connecting weight matrix $\{w_{ij}\}$ is chosen as:

$$w_{ij} = \begin{cases} -1, i \neq j \\ 0, i = j \end{cases} \quad (3)$$

It denotes that all the neuron oscillators are inhibitory with each other. The oscillating frequency of the rays is tuned by T_r and the oscillating amplitudes of the rays are tuned by c_i. The initial data of the CPG model is selected according to the method introduced in section 3.2.

In the braking mode, the thruster generates resistance by reversing the propagating orientation of the traveling wave. The characteristics of the oscillating wave in the braking mode are tuned similarly to them in the regular swimming mode. And the oscillating frequency should be higher than it in the regular swimming mode to produce a greater force.

In the rotational mode, the phases of the left five rays are same. The oscillating amplitudes gradually decrease from ray1 to ray5 and offset to one side of the centre of the thruster. The phases of the right five rays are also same and are opposite to them of the left five ones. The oscillating amplitudes gradually increase from ray6 to ray10 and offset to the other side. The sketch map of the movement of the rays is shown in Figure 11. With the relation of the phases and the bias of the amplitudes, the thruster can generate a stable clockwise or anti-clockwise torque. And with the variation of the amplitudes, the oscillating amplitude difference between adjacent rays will not be too big to destroy the motors. The connecting weight matrix $\{w_{ij}\}$ values as:

$$w_{ij} = \begin{cases} 1, |i-j| \leq 5, i \neq j \\ -1, |i-j| > 5, i \neq j \\ 0, i = j \end{cases} \quad (4)$$

The bias of the oscillating amplitude is tuned by d_i. Other characteristics are tuned similarly to the regular swimming mode.

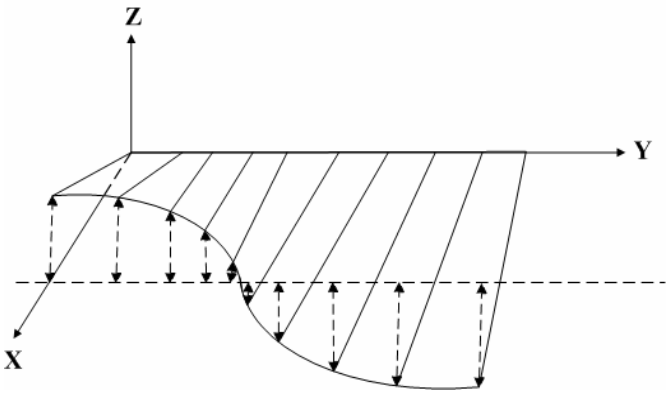

Fig. 11. The sketch of the movement of the rays.

The switch between two locomotion modes with reversed traveling waves should be done by tuning both of the parameters and the stable variables of the CPG model. Other cases of switch only need tuning the parameters.

4.3 Result of the experiment

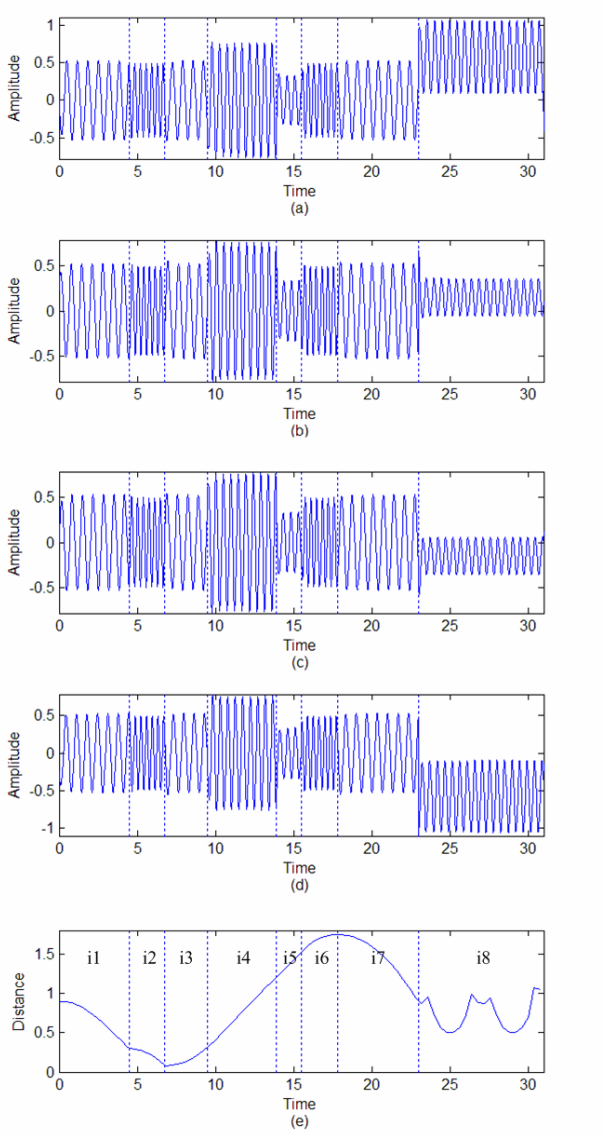

Fig.12.Experiment results: (a) Oscillating waves of ray1; (b) Oscillating waves of ray5; (c) Oscillating waves of ray6; (d) Oscillating waves of ray10; (e) distance information sent back from the laser sensor.

Because of the constraint in space, only the oscillating waves of ray1, ray5, ray6, ray10 are shown in Figure 12(a), (b), (c), and (d). Other rays have similar wave shapes. Distance information from the thruster to the sidewall of the tank, which is detected by the distance laser sensor, is shown in Figure 12(e). In interval i1, the thruster which is at rest in the middle of the tank starts to move toward one sidewall of the tank. When it moves 30 centimeters away from the sidewall, the infrared sensor detects the wall and the thruster switches to braking mode. In interval i2, the thruster decelerates to 0. And from interval i3 on, the thruster moves to the other sidewall of the tank. In interval i4 and i5, the thruster varies its oscillating frequency and amplitude. In interval i6, the thruster comes near to sidewall and brakes again. In interval i7, the thruster moves toward the middle of the tank. In the last interval, the thruster switches to rotational mode.

5. CONCLUSION

In this paper, we introduce a CPG based motion control approach for a biologically inspired underwater thruster with undulating long-fin. A method for phase control is proposed to adjust the oscillating phase of the motors which is used to drive the thruster. A CPG based controller is built to control the thruster. Different locomotion modes are obtained by tuning the parameters of the CPG model. And the switch between different modes is realized by the feedback of the sensors. The experiment at the end of this paper shows that the CPG based controller is valid to control the thruster.

ACKNOWLEGEMENT

This work is supported partly by NSFC (No.60605026, 60635010,50475179) and 863 program (No.2006AA11Z225).

REFERENCES

A.J. Ijspeert, A. Crespi (2007). Online trajectory generation in an amphibious snake robot using a lamprey-like central pattern generator model. *Robotics and Automation, IEEE Conf.* : 262-268.

Bradley G. Brewer, Ranu Jung (1997). Sensitivity analysis of a hybrid neural network for locomotor control in the lamprey. *Biomedical Engineering, IEEE Conf.*: 353-356.

Delcomyn F. (1980). Neural basis of rhythmic behavior in animals. *Science 210*:492-498.

J.J. Hu, M.M. Williamson, G.A. Pratt (1999). Bipedal locomotion control with rhythmic neural oscillators. *Intelligent Robots and Systems, IROS Proc.*: 1475-1481

Kimura H., Fukuoka Y., Mimura T (2005). Dynamics based integration of motion adaptation for a quadruped robot. *Adaptive motion of animals and machines*. Springer-Verlag, Tokyo: 215-224.

K. Izumi, A. Tajima, G.L. Liu, K. Watanabe (2006). The Design of Wave Shape for Coupled Van del Pol Oscillators, *SICE-ICASE Conf.*: 4220-4223.

Matsuoka K. (1985). Sustained oscillations generated by mutually inhibiting neurons withadaptation. *Biological Cybernetics,52*: 367-376.

M.J. Lighthill, R.W. Blake (1990). Biofluid dynamics of balistiform and gymnotiform locomotion. Part 1, Biological background and analysis by elongated-body theory. *J. Fluid Mech. 212*: 183–207.

M. Sfakiotakis, D.M. Lane, J.B.C. Davies (1999). Review of fish swimming modes for aquatic locomotion, *IEEE J. of Oceanic Engineering, Vol.24, No. 2*: 237-252.

Xiuli Zhang (2004). Biological-inspired rhythmic motion and environmental adaptability for quadruped robot. *Dissertation Submitted to Tsinghua University in partial fulfillment of the requirement for the degree of Doctor of Engineering*: 41-61.